NLTE effects of Ti I in M dwarfs and giants

Peter H. Hauschildt

Dept. of Physics and Astronomy, University of Georgia, Athens, GA 30602-2451 Email: yeti@hal.physast.uga.edu

and

Dept. of Physics and Astronomy, Arizona State University, Tempe, AZ 85287-1504

France Allard & David R. Alexander
Dept. of Physics, Wichita State University, Wichita, KS 67260-0032
E-Mail: allard@eureka.physics.twsu.edu & dra@twsuvm.uc.twsu.edu

E. Baron

Dept. of Physics and Astronomy, University of Oklahoma 440 W. Brooks, Rm 131, Norman, OK 73019-0225

E-Mail: baron@phyast.nhn.ou.edu

ABSTRACT

We present detailed NLTE Ti I calculations in model atmospheres of cool dwarf and giant stars. A fully self-consistent NLTE treatment for a Ti I model atom with 395 levels and 5279 primary bound-bound transitions is included, and we discuss the implication of departures from LTE in this atom for the strengths of Ti I lines and TiO molecular bands in cool star spectra. We show that in the atmospheric parameter range investigated, LTE is a poor approximation to Ti I line formation, as expected from the low collisional rates in cool stars. The secondary effects of Ti I overionization on the TiO number density and the TiO molecular opacities, however, are found to be negligible in the *molecular* line forming region for the relatively small parameter range studied in this paper.

1. Introduction

The opacity in the outer layers of the atmospheres of M stars are dominated by a small number of very strong molecular compounds (H₂O, TiO, H₂, CO, VO). Most of the hydrogen is locked in molecular H₂, most of the carbon in CO; and H₂O, TiO, and VO opacities define a pseudo-continuum covering the entire flux distribution of these stars. The optical "continuum" is due to TiO vibrational bands which are often used as temperature indicators for these stars. The indicators may be the depth of the bands relative to the

peaks between them; or the depth of the VO bands; or the strength of the atomic lines relative to the local "continuum"; or even the strength of the infrared water bands; all of these depend on the strength of the TiO bands and the amount of flux-redistribution to longer wavelengths caused by the blocking of the flux in the optical and near-IR by TiO. Departures from LTE of the Ti I atom, and thus indirect changes in the concentration of the important TiO molecule, could therefore have severe and measurable consequences on the atmospheric structure and spectra of cool stars (Johnson, 1994; Gustafsson & Jorgensen, 1994). Departures from LTE in the photospheres of cool stars have been investigated in detail in the line transfer and dissociative equilibrium of H₂ in red giant atmospheres (Lambert & Pagel, 1968; Vernazza, Avrett, & Loeser, 1981; Anderson, 1989). NLTE effects of CO have been investigated in the Sun (Thompson, 1973; Ayres & Wiedemann, 1989) and in red giant atmospheres (Carbon, Milkey, & Haesley, 1976; Wiedemann & Ayres, 1991; Wiedemann et al., 1994). These studies led to the conclusion that even after the passage of pulsationally driven shocks the recombination of H₂ and CO must proceed rapidly, leading to number densities very close to LTE values. Pavlenko et al. (1995) and Carlsson et al. (1995) showed that the equivalent widths of the Li I resonance lines are affected by NLTE effects and have derived NLTE curves of growth for a range of model parameters. Andretta. Doyle, & Byrne (1997) have performed NLTE calculations for Na I using a method similar to that of Carlsson et al. (1995). NLTE effects on the excitation potential and spectral lines of the much larger Ti atom have been analyzed in late-type giants by Ruland et al. (1980); Brown, Tomkin, & Lambert (1983).

Due to their very low electron temperatures, the electron density is extremely low in M stars; the absolute electron densities are even lower than found in low density atmospheres, such as those of novae and SNe. Collisions with particles other than electrons, e.g., H₂ or helium, are not as effective as electron collisions in restoring LTE, both because of their smaller cross-sections and their much smaller thermal velocities. Therefore, collisional rates which tend to restore LTE, could be very small in cool stars. This in turn could significantly increase the importance of NLTE effects in M stars when compared to, e.g., solar type stars with much higher electron densities and temperatures.

The NLTE treatment of molecules such as H_2O and TiO which have several million transitions is a formidable problem which requires an efficient method for the numerical solution of the multi-level NLTE radiative transfer problem. Classical techniques, such as the complete linearization or the Equivalent Two Level Atom method, are computationally prohibitive for large model atoms and molecules. Currently, the operator splitting or approximate Λ -operator iteration (ALI) method (e.g., Cannon, 1973; Rybicki, 1972, 1984; Scharmer, 1984) seems to be the most effective way of treating complex NLTE radiative transfer and rate equation problems. Variants of the ALI method have been developed to

handle complex model atoms, e.g., Anderson's multi-group scheme (Anderson, 1987, 1989) or extensions of the opacity distribution function method (Hubeny & Lanz, 1995). However, these methods have problems if line overlaps are complex or if the line opacity changes rapidly with optical depth, a situation which occurs in cool stellar atmospheres. The ALI rate operator formalism, on the other hand, has been used successfully to treat very large model atoms such as Fe directly and efficiently (cf. Hauschildt & Baron, 1995; Hauschildt et al., 1996; Baron et al., 1996).

In this paper we discuss NLTE effects of Ti I in fully self-consistent models for a few representative M dwarf and M giant model atmospheres and spectra.

2. Methods and Models

In order to investigate the importance of Ti I NLTE effects on the formation of cool star spectra, a full NLTE model calculation is required. This means that the multi-level NLTE rate equations must be solved self-consistently and simultaneously with the radiative transfer and energy equations, including the effects of line blanketing and of the molecular equation of state. For the purpose of this analysis we use our multi-purpose stellar atmosphere code PHOENIX originally developed for the modeling of the expanding atmospheres of novae and supernovae, and adapted to conditions found in cool stars by Allard and Hauschildt (1995, hereafter AH95). PHOENIX (version 8.0, Hauschildt et al., 1996; Hauschildt, Baron, & Allard, 1997) uses a spherical radiative transfer for giant models $(\log(q) < 3.5)$, and an equation of state (EOS) including more than 600 molecules. In all models TiO⁺ (and ZrO⁺) species are included in the equations of state according to partition functions published by Gurvich & Glushko (1982) for a consistent ionization equilibrium of Ti. For the strongest ca. 4×10^6 atomic & molecular lines, we use detailed depth-dependent Voigt profiles with improved damping constant computation (Schweitzer, 1995; Schweitzer et al., 1996), and Gaussian profiles for an additional 10⁷ much weaker lines. In addition, we include ca. 2000 photo-ionization cross sections for atoms and ions (Verner & Yakovley 1995). These and related improvements, as well as the resulting LTE "NextGen" model grids, are described in detail by Schweitzer (1995); Schweitzer et al. (1996) and Allard & Hauschildt (in preparation).

Both the NLTE and LTE lines for atoms and molecules are treated with a direct line-by-line method. We do *not* use pre-computed opacity sampling tables, and thereby allow for computation of pressure-dependent Voigt profiles, changes in the isotope ratios, and avoid possible interpolation effects. We dynamically select the relevant lines from master line lists at the beginning of each iteration and sum the contribution of every line within a

search window to compute the total line opacity at arbitrary wavelength points. The latter is crucial in NLTE calculations in which the wavelength grid is both irregular and variable (from iteration to iteration due to changes in the physical conditions). This approach also allows detailed and depth dependent line profiles to be used during the iterations. To make this method computationally efficient, we employ modern numerical techniques, e.g., vectorized and parallel block algorithms with high data locality (Hauschildt, Baron, & Allard, 1997), and we use on high-end workstations or supercomputers for the model calculations. In the calculations we present in this paper, we have set the micro-turbulent velocity ξ to $2 \,\mathrm{km} \,\mathrm{s}^{-1}$. We include LTE lines (i.e., lines of species that are not treated in NLTE) if they are stronger than a threshold $\Gamma \equiv \chi_l/\kappa_c = 10^{-4}$, where χ_l is the extinction coefficient of the line at the line center and κ_c is the local b-f absorption coefficient.

PHOENIX is a full multi-level NLTE code, i.e., NLTE effects are considered self-consistently in the model calculations, including the temperature corrections. The temperature corrections and the convection are treated as described in Allard & Hauschildt (1995). Hauschildt & Baron (1995) have extended the numerical method developed by Hauschildt (1993) for NLTE calculations with a very detailed model atom of Fe II. In this section we describe how we apply this technique to a detailed Ti I model atom from the list of NLTE species already available in the model calculations.

2.1. NLTE Calculational Method

The large number of transitions of the Ti I ion that have to be included in realistic models of the Ti I NLTE line formation require an efficient method for the numerical solution of the multi-level NLTE radiative transfer problem. As already mentioned, the Ti I model atom described here includes more than 5200 individual NLTE lines plus a large number of weak background transitions. Classical techniques, such as the complete linearization or the Equivalent Two Level Atom methods, are computationally prohibitive. In addition, we are also modeling moving media (e.g., stellar winds, novae and supernovae), therefore, approaches such as Anderson's multi-group scheme or extensions of the opacity distribution function method (Hubeny & Lanz (1995)) cannot be applied. Again, simple approximations such as the Sobolev method, are very inaccurate in problems in which lines overlap strongly and make a significant continuum contribution (important for weak lines), as is the case for nova (and SN) atmospheres (Hauschildt et al., 1996; Baron et al., 1996, cf.).

We use, therefore, the multi-level operator splitting method described by Hauschildt (1993). This method solves the non-grey, spherically symmetric, special relativistic equation

of radiative transfer in the co-moving (Lagrangian) frame using the operator splitting method described in Hauschildt (1992). Details of the method are also described in Hauschildt & Baron (1995), so we give here only a summary of the method.

Even with highly effective numerical techniques, the treatment of possibly more than one million NLTE lines poses a significant computational problem, in particular in terms of memory usage. In addition, most lines are very weak and do not contribute significantly to the radiative rates. However, together, they can influence the radiation field from overlapping stronger transitions and should be included as background opacity. Therefore, we separate the stronger "primary" lines from the weaker "secondary" lines by defining a threshold in $\log(gf)$, which can be arbitrarily changed. Lines with gf-values larger than the threshold are treated in detail, i.e., they are fully included as individual transitions in the radiative transfer (assuming complete redistribution) and rate equations. In addition, we include special wavelength points within the profile of the strong primary lines.

The secondary transitions are included as background NLTE opacity sources but are not explicitly included in the rate equations. Their cumulative effect on the rates is included, since the secondary lines are treated by line-by-line opacity sampling in the solution of the radiative transfer equation. Note that the distinction between primary and secondary transitions is only a matter of convenience and technical feasibility. It is not a restriction of our method or the computer code but can be easily changed by altering the appropriate input files. As more powerful computers become available, all transitions can be handled as primary lines by simply changing the input files accordingly. We do not pose additional thresholds such as the energy or the statistical weight of the lower level of a line. However, we include in the selection process only observed lines between known levels in order to include only lines with well known gf- values. All predicted lines of Kurucz are included as secondary lines (see Hauschildt & Baron, 1995) for completeness. For all primary lines the radiative rates and the "approximate rate operators" (Hauschildt, 1993) are computed and included in the iteration process.

2.2. The Ti I model atom

To construct the Ti I model atom we have selected the first 34 terms of Ti I. We include all observed levels that have observed b-b transitions with $\log{(gf)} > -3.0$ as NLTE levels where g is the statistical weight of the lower level and f is the oscillator strength of the transition. This leads to a model atom with 395 levels and 5279 primary transitions treated in detailed NLTE. That is, we solve the complete b-f & b-b radiative transfer and rate equations for all these levels including all radiative rates of the primary lines. A

Grotrian diagram of this model atom is shown in Fig. 1. In addition, we treat the opacity and emissivity for the remaining ≈ 0.8 million weak secondary b-b transitions in NLTE, if one level of a secondary transition is included in the model. A detailed description of the numerical method is presented in Hauschildt & Baron (1995).

Photo-ionization and collisional rates for Ti I are not yet available. Thus, we have taken the results of the Hartree Slater central field calculations of Reilman & Manson (1979) to scale the ground state photo-ionization rate and have then used a hydrogenic approximation for the energy variation of the cross-section. Although they are only very rough approximations, the exact values of the b-f cross-sections are not important for the opacities themselves which are dominated by known b-b transitions of Ti I and other species. They do, however, have an influence on the actual b-f rates but this remains unimportant for the computational method used in this work.

While collisional rates are important in hotter stellar atmospheres with high electron densities, they remain nearly negligible when compared to the radiative rates for the low electron densities found in cool stars. We have approximated bound-free collisional rates using the semi-empirical formula of Drawin (1961). The bound-bound collisional rates are approximated by the semi-empirical formula of Allen (1973), while the Van Regemorter's formula (1962) was used for permitted transitions.

A more accurate treatment of this model atom requires the availability of more accurate collisional and photo-ionization rates for Ti I. In the present calculations we have neglected collisions with particles other than electrons because the cross-sections are basically unknown. Additional collisional processes would tend to restore LTE, therefore, the NLTE effects that we obtain in our calculations should be maximized.

3. Results

We have computed a small number of both giant and dwarf models to investigate the effects of Ti NLTE on the structure and the spectra of cool stars. The giant models are computed using the spherically symmetric, static mode of PHOENIX, while the dwarf models use the plane-parallel mode. For the three giants we use a gravity of $\log(g) = 1.0$, solar abundances and the following $T_{\rm eff} = 3200\,\mathrm{K}$, $3600\,\mathrm{K}$, and $4000\,\mathrm{K}$. All giant models have radial extensions of less than 10%. In addition, we computed two NLTE dwarf models with $\log(g) = 5.0$, solar abundances and $T_{\rm eff} = 2700\,\mathrm{K}$ and $4000\,\mathrm{K}$ for comparison. All models include the Ti I NLTE treatment as discussed above as well as the standard PHOENIX equation of state (NLTE mode) and additional LTE background lines (about 10–15 million

atomic and molecular lines). The NLTE effects are included in both the temperature iterations (so that the structure of the models includes NLTE effects) and all radiative transfer calculations. With the exception of the hottest models, the majority of the line opacity comes from the LTE TiO and water wapor lines in most layers of the models, however, the Ti I lines are an important source of opacity in some of the outer laters of the models, in particular in the hotter models. For Ti I primary lines we use 5 to 11 wavelength points within their profiles. This procedure typically leads to about 150,000 wavelength points for both the model iteration and the synthetic spectrum calculations.

3.1. Departure coefficients for Ti I

In Figs. 2—4 we show the departure coefficients of Ti I for the three giant models. Figures 5 and 6 show the corresponding results for the two dwarf models. The optical depth scale, $\tau_{\rm std}$, is measured in the b-f and f-f continuum at $1.2\mu m$. Note that the atmospheres are *extremely* non-grey, some Ti I lines form at $\tau_{\rm std} \approx 10^{-6}$. Therefore, we show in the following graphs a large dynamical range of standard optical depth.

The departure coefficients in the dwarf models are significantly smaller than in the giant models, by several orders of magnitude. This is mostly an ionization effect, in the dwarf models Ti I and Ti molecules (mainly TiO) have higher concentrations relative to Ti II than in the giant models (see below). The electron temperatures in the outer regions of the dwarfs and giants are comparable. Therefore, the departure coefficients b_i are distinctly different since their definition explicitly includes the concentrations of both electrons and Ti II (cf. Mihalas, 1978, p. 219).

For the giant models, the $T_{\rm eff}=3600\,{\rm K}$ model has the smallest spread of the departure coefficients compared to the 3200 K and 4000 K models, indicating the smallest "internal" NLTE effects for this model. The range of the b_i 's in all giant models is about a factor of 10 at $\tau_{\rm std}=10^{-6}$, but the line forming regions are farther inward, roughly between $\tau_{\rm std}=10^{-4}$ and $\tau_{\rm std}=1$. For most of the Ti I levels, the departure coefficients are less than unity, however at lower effective temperatures more levels show $b_i>1$ in the outer part of the atmosphere. Typically, $b_i<1$ can be associated with an overionization of Ti I relative to the LTE state. However, this is valid *only* if the electron densities of the NLTE and LTE cases are very similar, otherwise the behavior is more complicated (Hauschildt et al., 1996). In the models presented here, the electron densities of the LTE and NLTE models are basically identical because we have intentionally treated the important electron denors (mostly alkali and earth-alkali metals) in LTE.

The spread of the departure coefficients is much larger in the dwarf models, in particular for the cooler model. However, the large electron pressures in the dwarfs will compensate for the effect of the departures from LTE and result in smaller changes in the Ti I line profiles, as we discuss below.

3.2. NLTE effects on balance of Ti I, II and Ti-molecules

To analyze the effects of Ti I NLTE on the formation of the important TiO molecule, the major opacity source in the optical spectra of cool stars, we plot the relative concentration $P_i/P_{\rm gas}$ of a variety of Ti ions and molecules for both the LTE and the NLTE cases in Figs. 7—11. The LTE figures were constructed by using the NLTE structure of the model atmosphere but setting all $b_i = 1$. The LTE and NLTE structures are very similar out to $\tau_{\rm std} \approx 10^{-7}$, in the very outer regions the NLTE models are up to 300K cooler than their LTE counterparts due to increased line cooling. Therefore, we have used the NLTE structures exclusively in these figures in order to avoid the effects of the cooler outer layers on the plots.

The main differences between the giant and the dwarf models are caused by higher pressures in the dwarf models compared to the giants. This results in Ti II being more important in the giants than in the dwarfs (compare Figs. 9 and 11). The higher pressures in dwarfs also cause much higher concentrations of Ti-molecules in dwarfs than in giants of comparable effective temperatures.

Comparison of the LTE and NLTE results for the same effective temperatures shows that for the giants the effects on the concentration of Ti species is relatively small for $T_{\rm eff}=3200\,{\rm K}$. Only for $\tau_{\rm std}\leq 10^{-4}$ do NLTE effects on the EOS become noticeable. The main effect is that the concentration of Ti I is smaller, whereas the concentration of Ti II and TiO⁺ are slightly higher than in the LTE model. The concentration of TiO is hardly changed by NLTE effects in this particular model, only in the outermost optically very thin regions does the TiO concentration drop, with a maximum change of about a factor of 2.

The results are similar for the $T_{\rm eff}=3600\,{\rm K}$ giant model. Here, NLTE effects prevent recombination of Ti II to Ti I in the very outer parts of the atmosphere. However, the optical depths there are very small and the effects on the spectrum due to the EOS NLTE effects are quite small. As in the $T_{\rm eff}=3200\,{\rm K}$ model, the TiO concentration is reduced but the TiO⁺ concentration is increased in the regions where NLTE effects are important for the EOS. The $T_{\rm eff}=4000\,{\rm K}$ giant model reacts similarly to the 3600 K model, but at this effective temperature Ti II is the dominant Ti-species even throughout the LTE

atmosphere.

In the dwarf models, the situation is very different. The higher pressures favor molecules over atoms and ions, which impacts the effect of Ti I NLTE on the structure. The NLTE $T_{\rm eff} = 2700\,\rm K$ model shows increases in the concentrations of TiO⁺ and Ti II for $\tau_{\rm std} < 10^{-2}$ but virtually no change in the concentrations of the dominant TiO and TiO₂ molecules. Note the TiO⁺ increases more than the Ti II concentration, indicating that the additional Ti II initially created by NLTE overionization of Ti I is converted into TiO⁺.

The $T_{\rm eff}=4000\,{\rm K}$ dwarf model shows a somewhat different behavior. In this model, the NLTE effects increase the concentration of Ti II below $\tau_{\rm std}\approx 10^{-5}$ significantly so that Ti II is the dominant Ti-species below $\tau_{\rm std}\approx 10^{-6}$, whereas in the LTE model TiO becomes the dominant species below $\tau_{\rm std}\approx 10^{-7}$. NLTE effects reduce the overall concentration of Ti-molecules, but increase the relative importance of TiO⁺.

All changes in Ti-molecules occur at small optical depths in the outer regions of the model atmospheres. Considering the fact that the molecular lines form deeper in the atmosphere than the atomic lines, this indicates that the effects of atomic Ti NLTE on the lines of Ti-molecules will be very small.

3.3. NLTE effects on Ti I line profiles in M Star Spectra

The influence of NLTE effects on the formation and emergent profiles of the Ti I lines can be estimated from the run of the ratio of the line source function S_L to the local Planck-function versus the optical depth. This is shown in a series of overview plots in Figs. 12—16 for all models. The large number of Ti I lines in NLTE masks individual transitions, but the figures show the wide range that S_L/B spans for the different transitions. In general, the lines become optically thin for a wide range of optical depths, between $\tau_{\rm std} \approx 10^{-5}$ and unity. The electron temperatures and thus the Planck-function drop rapidly with smaller optical depths, creating large S_L/B ratios in the outer atmosphere. This indicates that S_L has decoupled completely from the thermal pool above the line forming region of each line, as expected.

The S_L/B ratio is overall closest to unity, its LTE value, for the $T_{\rm eff}=3600\,{\rm K}$ giant model. Therefore, this model should show the smallest changes in line profiles of the three giant models. However, even in this model many lines have S_L/B ratios very different from unity, therefore a number of Ti I lines will be different from the LTE case. For many transitions, the ratio S_L/B is less than unity in the line forming region, indicating that the absorption lines will show deeper cores than in the LTE case. Note that this effect combines

with the effects of the Ti-NLTE on the EOS, which for the models discussed here generally reduces the concentration of Ti I, in part canceling the effects due to NLTE scattering.

We demonstrate the net effect of NLTE on the formation of Ti I lines in giants in Figs. 17 to 19. As expected, NLTE effects are smallest for the model with $T_{\rm eff}=3600$. In the optical spectral region, the changes caused by the Ti I NLTE line formation are very small and would be hard to observe due to the enormous crowding of lines in this spectral region. NLTE effects for the same Ti I lines are smaller for dwarfs at similar effective temperature, cf. Figs. 20 and 21.

In the cooler models, the Ti I lines form deeper in the atmosphere in a region in which the radiation field is nearly Planckian and thus NLTE effects are very small. This is due to the enormous background opacity of TiO and other molecules. In the outer atmosphere of the cooler models the concentration of Ti I is much smaller than that of TiO, thus the effect of the large departures from LTE that we find in these regions on the Ti I line profiles is very small.

In the hotter dwarf models, NLTE effects, in particular on the near-IR lines, are larger. The giant models, however, show an opposite behavior (the NLTE effects on the Ti I lines are larger for the cooler models). In these models the line forming region of the Ti I lines is inside the region in which departures from LTE are significant. In addition, the TiO opacity is relatively smaller than in the cooler models. For the Ti I line at $\lambda_{\rm vac} \approx 9641 {\rm \AA}$, NLTE effects make the core of the line deeper than the LTE model predicts. This is due to line scattering which removes photons from the line core and re-distributes them into the line wings. These effects are present in most Ti I lines, but there are a few exceptions in the giant model with $T_{\rm eff} = 4000$ for which some lines are weaker in NLTE than in LTE (cf. Fig. 19). Abundance determinations of Ti, or likely all metals, from near-IR or IR lines should therefore include NLTE effects wherever possible.

4. Summary and Conclusions

For the model parameters that we have considered so far, effects of Ti I NLTE on the TiO bands are very small. This seems to be due to the fact that the line forming region of TiO (around $\tau_{\rm std} \approx 10^{-2}$) is inside of the line forming region of the Ti I lines. Therefore, the TiO lines form in a region in which the Ti I atom is basically in LTE and Ti I NLTE effects that are important at smaller optical depths cannot affect TiO lines significantly. The situation is different for the TiO⁺ molecule which forms from Ti II and O I (cf. Fig. 10). This molecule is very sensitive to Ti I NLTE effects and its lines would be helpful indicators

of Ti I NLTE effects.

In further investigations it will be very interesting to look for NLTE effects in the TiO line formation itself. This is certainly feasible with modern numerical techniques once adequate data for TiO are available. In addition, NLTE effects of carbon, nitrogen, oxygen, Ti I–II and, in hotter models, Fe I–II need to be investigated in detail for larger grid of models to assess the impact of NLTE on model structures and spectra over wide regions of the Hertzsprung-Russell diagram. We are currently preparing such models and will report the results elsewhere (Hauschildt et al, in preparation).

Acknowledgments: It is a pleasure to thank H.R. Johnson, S. Starrfield, and S. Shore for stimulating discussions. We also thank the referee for helpful comments that helped us improving the paper. This work was supported in part by NASA ATP NAGW 5-3618 and LTSA NAGW 5-3619 grants to UGA, by NASA LTSA grants NAGW 4510 and NAGW 2628, NASA ATP grant NAG 5-3067 to Arizona State University, by NSF grant AST-9417242 and an IBM SUR grant to University of Oklahoma; as well as by NSF grant AST-9217946 to Indiana University and by NASA LTSA grant NAG 5-3435 and a NASA EPSCoR grant to Wichita State University. Some of the calculations presented in this paper were performed at the San Diego Supercomputer Center (SDSC) and the Cornell Theory Center (CTC), with support from the National Science Foundation, and at the NERSC with support from the DoE. We thank all these institutions for a generous allocation of computer time.

REFERENCES

Allard, F., & Hauschildt, P. H. 1995, ApJ, 445, 433.

Allen, C. W. 1973, Astrophysical Quantities, Athlone Press, London, third edition.

Anderson, L. S. 1987, In *Numerical Radiative Transfer*, W. Kalkofen, editor, page 163, Cambridge University Press.

Anderson, L. S. 1989, ApJ, 339, 559.

Andretta, V., Doyle, J. G., & Byrne, P. B. 1997, A&A, in press.

Ayres, T. R., & Wiedemann, G. R. 1989, ApJ, 338, 1033.

Baron, E., Hauschildt, P. H., Nugent, P., & Branch, D. 1996, MNRAS, 283, 297.

Brown, J. A., Tomkin, J., & Lambert, D. L. 1983, ApJ, 265, L93.

Cannon, C. J. 1973, JQSRT, 13, 627.

Carbon, D. F., Milkey, R. W., & Haesley, J. N. 1976, ApJ, 207, 253.

Carlsson, M., Rutten, R. J., Bruls, J. H. M. J., & Shchukina, N. G. 1995, A&A, in press.

Drawin, H. W. 1961, Zs. f. Phys., 164, 513.

Gurvich, L., & Glushko, V. 1982, Thermodinamicheskie Svoistva Individual'nikh Veschev, 4 (Moscow: Sovit Acad. Sci.).

Gustafsson, B., & Jorgensen, U. G. 1994, A&A Rev., 6, 19.

Hauschildt, P., Baron, E., Starrfield, S., & Allard, F. 1996, ApJ, 462, 386.

Hauschildt, P. H. 1992, JQSRT, 47, 433.

Hauschildt, P. H. 1993, JQSRT, 50, 301.

Hauschildt, P. H., & Baron, E. 1995, JQSRT, 54, 987.

Hauschildt, P. H., Baron, E., & Allard, F. 1997, ApJ, in press.

Hubeny, I., & Lanz, T. 1995, ApJ, 439, 875.

Johnson, H. R. 1994, Effects of non-local thermodynamic equilibrium (nlte) on molecular opacities, In *Molecular Opacities in the Stellar Environment*, P. Thejll and U. Jørgensen, editors, I.A.U. Colloquium 146, Lecture Notes in Physics 438, pages 234–249, Springer-Verlag, Berlin.

Lambert, D. L., & Pagel, B. E. J. 1968, MNRAS, 141, 299.

Mihalas, D. 1978, Stellar Atmospheres, Freeman, San Francisco, 2 edition.

Pavlenko, Y. V., Rebolo, R., Martin, E. L., & Garcia-Lopez, R. J. 1995, A&A, in press.

Reilman, R. F., & Manson, S. T. 1979, ApJ Suppl., 40, 815.

Ruland, F., Holweger, H., Griffin, R., & Biehl, D. 1980, A&A, 92, 70.

Rybicki, G. B. 1972, In *Line Formation in the Presence of Magnetic Fields*, . G. Athay, L. L. House, and G. Newkirk Jr., editors, page 145, High Altitude Observatory, Boulder.

Rybicki, G. B. 1984, In *Methods in Radiative Transfer*, W. Kalkofen, editor, page 21, Cambridge Univ. Press.

Scharmer, G. B. 1984, In *Methods in Radiative Transfer*, W. Kalkofen, editor, page 173, Cambridge Univ. Press.

Schweitzer, A. 1995, *Modellatmosphäeren für M-Zwerge*, Master's thesis, University of Heidelberg.

Schweitzer, A., Hauschildt, P. H., Allard, F., & Basri, G. 1996, MNRAS, 283, 821.

Thompson, R. I. 1973, ApJ, 181, 1039.

Van Regemorter, H. 1962, ApJ, 136, 906.

Vernazza, J. E., Avrett, E. H., & Loeser, R. 1981, ApJS, 45, 635.

Verner, D. A., & Yakovlev, D. G. 1995, A&AS, 109, 125.

Wiedemann, G. R., & Ayres, T. R. 1991, ApJ, 366, 277.

Wiedemann, G. R., Ayres, T. R., Jennings, D. E., & Saar, S. H. 1994, ApJ, 423, 806.

Fig. 1.— Simplified Grotrian diagram of our Ti I model atom. All 395 levels and 5379 primary (i.e., full NLTE) lines are shown but the 0.8 million secondary (approximate) NLTE lines have been omitted for clarity.

5. Figures

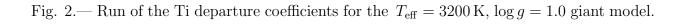


Fig. 3.— Run of the Ti departure coefficients for the $T_{\rm eff}=3600\,{\rm K},\,\log g=1.0$ giant model.

Fig. 4.— Run of the Ti departure coefficients for the $T_{\rm eff}=4000\,{\rm K},\,\log g=1.0$ giant model.

Fig. 5.— Run of the Ti departure coefficients for the $T_{\rm eff}=2700\,{\rm K},\,\log g=5.0$ dwarf model.

Fig. 6.— Run of the Ti departure coefficients for the $T_{\rm eff}=4000\,{\rm K},\,\log g=5.0$ dwarf model.

Fig. 7.— NLTE effects on the Ti ionization and molecule formation for the $T_{\rm eff} = 3200\,{\rm K}$, $\log g = 1.0$ giant model. The thin lines and symbols give the results for the LTE model, whereas the thick lines and symbols give the results for corresponding NLTE model.

Fig. 8.— NLTE effects on the Ti ionization and molecule formation for the $T_{\rm eff} = 3600 \, \rm K$, log g = 1.0 giant model. The thin lines and symbols give the results for the LTE model, whereas the thick lines and symbols give the results for corresponding NLTE model.

Fig. 9.— NLTE effects on the Ti ionization and molecule formation for the $T_{\rm eff} = 4000 \, \rm K$, log g = 1.0 giant model. The thin lines and symbols give the results for the LTE model, whereas the thick lines and symbols give the results for corresponding NLTE model.

- Fig. 10.— NLTE effects on the Ti ionization and molecule formation for the $T_{\text{eff}} = 2700 \,\text{K}$, $\log g = 5.0$ dwarf model. The thin lines and symbols give the results for the LTE model, whereas the thick lines and symbols give the results for corresponding NLTE model.
- Fig. 11.— NLTE effects on the Ti ionization and molecule formation for the $T_{\text{eff}} = 4000 \,\text{K}$, $\log g = 5.0$ dwarf model. The thin lines and symbols give the results for the LTE model, whereas the thick lines and symbols give the results for corresponding NLTE model.
- Fig. 12.— Line source functions for all Ti I NLTE lines for a giant model with the parameters $T_{\rm eff} = 3200\,{\rm K}$, $\log g = 1.0$.
- Fig. 13.— Line source functions for all Ti I NLTE lines for a giant model with the parameters $T_{\rm eff} = 3600\,{\rm K},\,\log g = 1.0.$
- Fig. 14.— Line source functions for all Ti I NLTE lines for a giant model with the parameters $T_{\text{eff}} = 4000 \,\text{K}$, $\log g = 1.0$.
- Fig. 15.— Line source functions for all Ti I NLTE lines for a dwarf model with the parameters $T_{\rm eff} = 2700 \, \text{K}$, $\log g = 5.0$.
- Fig. 16.— Line source functions for all Ti I NLTE lines for a dwarf model with the parameters $T_{\rm eff} = 4000 \, \text{K}$, $\log g = 5.0$.
- Fig. 17.— NLTE effects on the Ti I line at $\lambda_{\rm vac} \approx 9641 \text{Å}$ and around 5020 Å for a giant model with the parameters $T_{\rm eff} = 3200 \, \text{K}$, $\log g = 1.0$. The LTE spectrum (dotted curve) uses the same model structure as the NLTE spectrum (full curve) but with all departure coefficients set to unity. The fluxes are in arbitrary units.
- Fig. 18.— NLTE effects on the Ti I line at $\lambda_{\rm vac} \approx 9641 \text{Å}$ and around 5020 Å for a giant model with the parameters $T_{\rm eff} = 3600 \, \text{K}$, $\log g = 1.0$. The LTE spectrum (dotted curve) uses the same model structure as the NLTE spectrum (full curve) but with all departure coefficients set to unity. The fluxes are in arbitrary units.
- Fig. 19.— NLTE effects on the Ti I line at $\lambda_{\rm vac} \approx 9641 \text{Å}$ and around 5020 Å for a giant model with the parameters $T_{\rm eff} = 4000 \, \text{K}$, $\log g = 1.0$. The LTE spectrum (dotted curve) uses the same model structure as the NLTE spectrum (full curve) but with all departure coefficients set to unity. The fluxes are in arbitrary units.

Fig. 20.— NLTE effects on the Ti I line at $\lambda_{\rm vac} \approx 9641 {\rm \AA}$ and around 5020 Å for a dwarf model with the parameters $T_{\rm eff} = 2700 \, {\rm K}$, $\log g = 5.0$. The LTE spectrum (dotted curve) uses the same model structure as the NLTE spectrum (full curve) but with all departure coefficients set to unity. The fluxes are in arbitrary units.

Fig. 21.— NLTE effects on the Ti I line at $\lambda_{\rm vac} \approx 9641 \text{Å}$ and around 5020 Å for a dwarf model with the parameters $T_{\rm eff} = 4000 \, \text{K}$, $\log g = 5.0$. The LTE spectrum (dotted curve) uses the same model structure as the NLTE spectrum (full curve) but with all departure coefficients set to unity. The fluxes are in arbitrary units.